Support Information

First-principles study of photocatalytic performance of bismuth bromide oxide-based catalysts

[a] School of Light Industry & Chemical Engineering, Dalian Polytechnic University, No.1 Qinggongyuan, Ganjingzi District, Dalian 116034, People's Republic of China

[b] School of Physics and Electronic Information, Yan’an University, Yan’an 716000, China

[c] Science and Technology on Aerospace Chemical Power Laboratory, Laboratory of Emergency Safety and Rescue Technology, Hubei Institute of Aerospace Chemotechnology, Xiangyang 441003, China

[d] Division of Research and Development, 1277 Lovely Professional University, 144411 Phagwara, India

[e] Department of Physics Faculty of Engineering and Technology, SRM Institute of Science and Technology, Vadapalani Campus, Chennai-600026, Tamilnadu, India

[f] Department of Physics, Saveetha School of Engineering, Saveetha Institute of Medical and Technical Sciences (SIMATS), Thandalam, Chennai, Tamil Nadu 602105, India

[g] College of Science, University of Shanghai for Science and Technology, Shanghai 200093, People's Republic of China

* Corresponding author, E-mail addresses: (H. Ma) m-h-c@sohu.com (F. Zhang) yadxzfc@yau.edu.cn (Q. Zhang) qiangzhang@usst.edu.cn (X. Liu) liuxinghui119@gmail.com

In this study, we used a first-principles-based computational approach to calculate the catalytic performance of $Bi_xO_yBr_z$, specifically using the Vienna Ab initio Computational Simulation Package (VASP) combined with Density Functional Theory (DFT). For the treatment of the interaction of electron exchange and correlation coefficients, we have chosen the generalized gradient approximation (GGA-PBE) proposed by Perdue, Burke and Enzel. In the framework of the projector, we applied the method of augmented waves (PAW) and set the cutoff energy to 500 eV, choosing a plane wave basis set. In addition, we ensure that the energy convergence criterion reaches 1×10^{-4} eV/atom and that the residual force on any atom is less than 0.03 eV to guarantee the accuracy and reliability of the computational results.

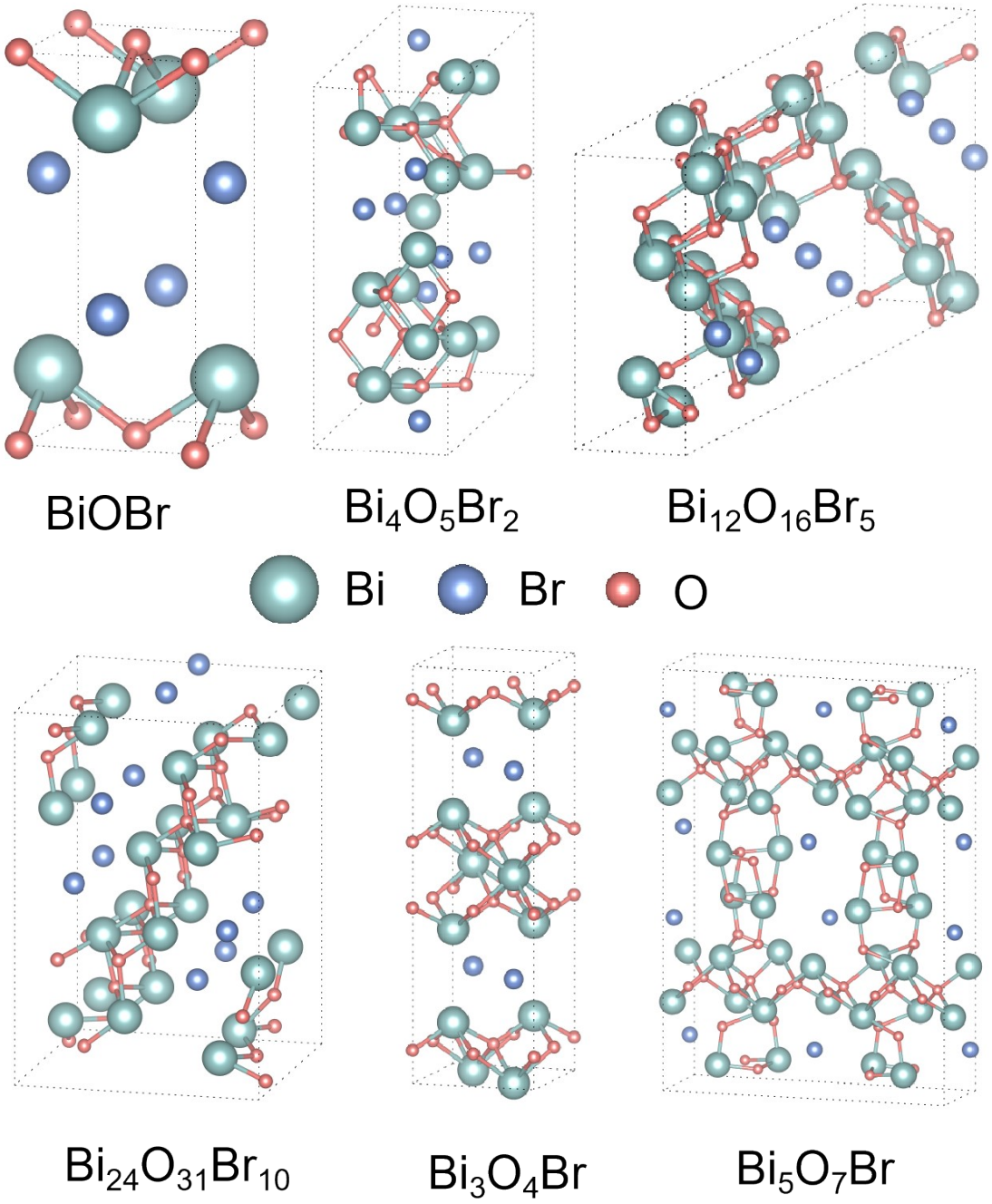

Figure S1 Initial cell structures of BiOBr, Bi_2OBr_2, Bi_3O_4Br, $Bi_4O_5Br_2$, Bi_5O_7Br, $Bi_{12}O_{16}Br_5$, $Bi_{24}O_{31}Br_{10}$.

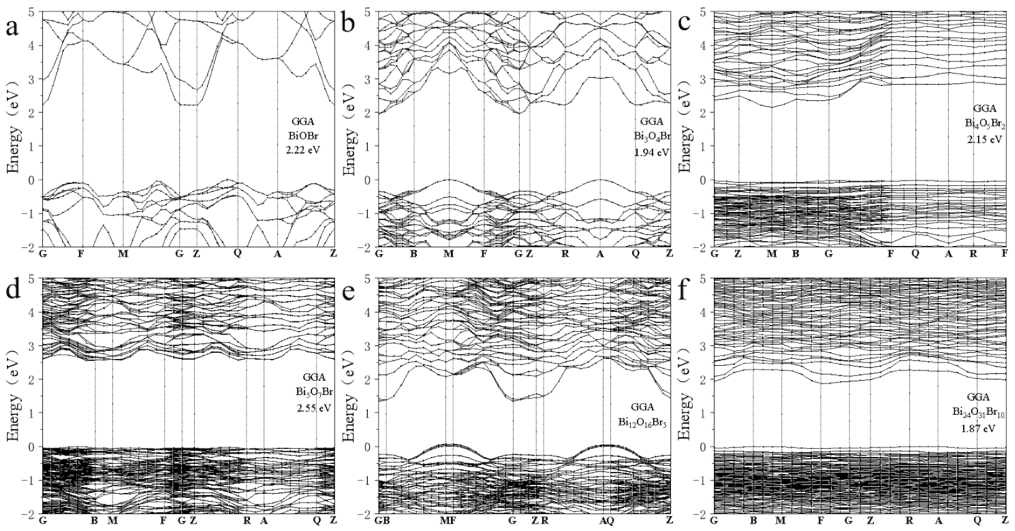

Figure S2 GGA-PBE functional calculated energy bands.

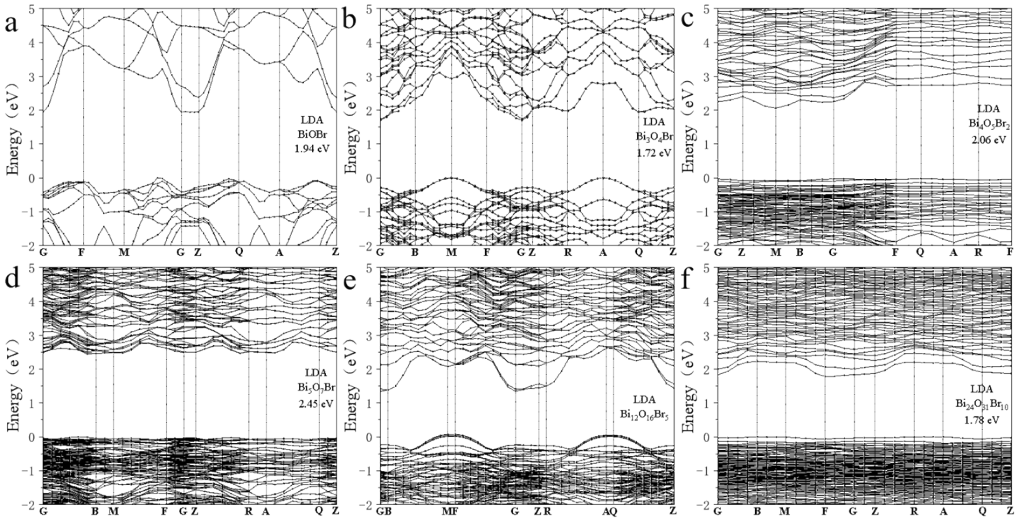

Figure S3 LDA CA-PZ functional calculated energy bands.

Table S1 The calculated lattice parameters and relative errors (%) using first-principlescompared with the experimental data.

Lattice Parameters	a/Å	b/Å	c/Å	V/Å^3	Error(%)
BiOBr[1]	3.794	3.923	8.092	124.535	3.6~3.9
Bi_2OBr_2	-	-	-	-	-
Bi_3O_4Br[2]	5.705	5.693	18.949	615.501	0.3~1.9
$Bi_4O_5Br_2$[3]	10.782	5.605	14.539	870.6	0.4~2.6
Bi_5O_7Br[4]	5.296	16.087	23.022	1961.6	2.3~8.6
$Bi_{12}O_{16}Br_5$	-	-	-	-	-
$Bi_{24}O_{31}Br_{10}$[5]	4.008	10.13	29.97	1217.5	0.5~7.6

Table S2 Band gap and UV-vis absorption of BiOBr.

Sample	Gap(eV)	UV-vis(nm)	Ref
Ag/BiOBr	2.95	420	[6]
BiOBr/BiOCl	2.94	421	[7]
IBP-BiOBr	2.85	435	[8]
BiOBr/lignin-biocha composites	2.65	442	[9]
BiOBr-OV	2.58	445	[10]
BiOBr/BiOCl/C	~2.68	~460	[11]
TiO_2-BiOBr	~3.16	~392	[12]
BiOBr/Bi	2.85	435	[13]
BiOBr/$Bi_{12}O_{15}C_{l6}$	2.59	~479	[14]
BiOBr(MP)	2.68	430	[15]
BiOBr(NS)	2.73	426	[15]
C/BiOBr	~2.72	~456	[16]
Bi/BiOBr-OV	2.59	425	[17]
GO/CDots/BiOBr	2.86	435	[18]
BiOBr-based	2.78	~446	[19]
Bi/BiOBr/AgBr	2.7	~459	[20]
Ag/AgBr/BiOBr	2.65	~468	[21]
BiOBr-OV microspheres	2.34	~530	[22]
BiOBr/Ti_3C_2	2.88	430	[23]
Ag-BiOBr-rGO	2.92	425	[24]

MWCNT/BiOBr	**2.8**	**~443**	[25]
BiOBr/$BiPO_4$	**2.52**	**~492**	[26]
Bi/BiOBr	**2.7**	**~459**	[27]
BiOBr	**2.75**	**~451**	[28]
AgBr-Ag-BiOBr	**2.8**	**~443**	[29]
BN/BiOBr	**2.78**	**~446**	[30]
BiOBr-square	**2.68**	**460**	[31]
BiOBr-circle	**2.82**	**440**	[31]
BiOBr/CQDs	**~2.82**	**~440**	[32]
BiOBr-(001)	**2.7**	**~440**	[33]
BiOBr-(010)	**2.73**	**~430**	[33]
up-conversion phosphors/BiOBr	**2.81**	**~441**	[34]
BiOBr/UiO	**2.64**	**443**	[35]
CdS/BiOBr	**2.77**	**447**	[36]
BiOBr/Bi_2WO_6	**2.57**	**~482**	[37]
OVs-BiOBr-30	**2.89**	**~429**	[38]
MIL-125(Ti)/BiOBr	**2.66**	**426**	[39]
BiOBr/$ZnWO_4$	**2.87**	**450**	[40]
$CaCO_3$-BiOBr	**2.7**	**416**	[41]
BN/BiOBr-1	**2.86**	**~434**	[42]
Fe-MOF- BiOBr	**3.06**	**~405**	[43]
BiOBr-Bi_2S_3	**2.87**	**420**	[44]

Cu-BiOBr	2.9	~428	[45]
BN/BiOBr-2	2.8	443	[46]
2D/2D BiOBr/CDs/g-C_3N_4	2.64	460	[47]
BiOBr/$La_2Ti_2O_7$	2.78	430	[48]
Ag@$BiPO_4$/BiOBr/$BiFeO_3$	2.5	450	[49]
CoAl-LDH/BiOBr	2.69	440	[50]
Bi_3O_4Br-BiOBr	2.7	430	[51]
Bi_5O_7Br/BiOBr	2.8	442	[52]
BiOBr@$Bi_4O_5Br_2$@Bi_5O_7Br	2.86	~434	[53]

Table S3 Band gap and UV-vis absorption of $Bi_4O_5Br_2$.

Sample	Gap(eV)	UV-vis(nm)	Ref
$Bi_4O_5Br_2$/$Bi_{24}O_{31}Br_{10}$	2.53	499	[54]
BiOBr@$Bi_4O_5Br_2$@Bi_5O_7Br	2.28	544	[53]
$Bi_4O_5Br_2$-UN	2.64	469	[55]
CDs/$Bi_4O_5Br_2$	2.41	455	[56]
Ag/AgBr/$Bi_4O_5Br_2$	2.4	517	[57]
I-$Bi_4O_5Br_2$	2.62	486	[58]
$Bi_4O_5Br_2$	2	~620	[59]
CdS/$Bi_4O_5Br_2$	2.31	537	[60]

$Bi_4O_5Br_2$/g-C_3N_4	2.98	~416	61
$Bi_4O_5Br_2$-GO	2.26	450	62
$Bi_4O_5Br_2$-1	2.28	~544	63
$Bi_4O_5Br_2$ NSV	2.42	~512	64
$Bi_4O_5Br_2$/g-C_3N_4-1	2.18	550	65
$Bi_4O_5Br_2$/ZIF-8	2.16	570	66
$Bi_4O_5Br_2$@GO	2.63	471	67
Bi-$Bi_4O_5Br_2$	2.38	~521	68
$Bi_4O_5Br_2$ nanosheets	2.33	~532	69
$Bi_4O_5Br_2$ Nano	2.37	~523	70
$Bi_4O_5Br_2$ BC	2.31	~537	71
AgI/$MoSe_2$/$Bi_4O_5Br_2$	2.62	474	72
$Bi_4O_5Br_2$@TiO_2	2.45	~506	73
$Bi_4O_5Br_2$-I	2.46	503	74
3D flower-sphere $Bi_4O_5Br_2$	2.45	492	75
WO_3/$Bi_4O_5Br_2$	2.27	~546	76
Bi-based $Bi_xO_yBr_z$($Bi_4O_5Br_2$)	2.57	483	77
Bi_2S_3/$Bi_4O_5Br_2$	2.53	~490	78
$Bi_4O_5Br_2$/graphene	2.54	~488	79
$Bi_4O_5Br_2$/ AgBr	2.53	490	80
Bi plasmonic/$Bi_4O_5Br_2$	2.41	~515	81
3D $Bi_4O_5Br_2$	2.5	490	82

$Bi_4O_5Br_2$-MoS_2	2.43	~510	[83]
$Bi_4O_5Br_2$/$Bi_4O_5I_2$/Fe_3O_4	2.53	490	[84]
$Bi_4O_5Br_2$-Bi	2.21	470	[85]
$Bi_4O_5Br_2$/$Mn_xZn_{1-x}Fe_2O_4$	2.43	~510	[86]
$Bi_4O_5Br_2$ g-C_3N_5	2.62	~473	[87]
Fe-$Bi_4O_5Br_2$	2.26	500	[88]
CuTCPP/$Bi_4O_5Br_2$	2.25	~551	[89]
$Bi_4O_5Br_2$-OVs	2.44	~508	[90]
Bi/$Bi_4O_5Br_2$	2.25	~551	[91]
$Bi_{12}O_{17}Br_2$/$Bi_4O_5Br_2$	2.71	440	[92]
$Bi_4O_5Br_2$/α-MnS	2.29	~541	[93]
$Bi_4O_5Br_2$/NH_2-MIL-125(Ti)	2.25	500	[94]

Table S4 Band gap and UV-vis absorption of $Bi_{24}O_{31}Br_{10}$.

Sample	Gap(eV)	UV-vis(nm)	Ref
Bi_3O_4Br-$Bi_{24}O_{31}Br_{10}$	2.07	550	[95]
$Bi_4O_5Br_2$/$Bi_{24}O_{31}Br_{10}$	2.5	514	[54]
$Bi_{24}O_{31}Br_{10}$ NBs	2.4	~517	[96]
$Bi_{24}O_{31}Br_{10}$ NSs	2.47	~502	[96]

AgI-$Bi_{24}O_{31}Br_{10}$	**2.53**	**491**	**97**
$Bi_{24}O_{31}Br_{10}(OH)\delta$	**~2.5**	**~496**	**98**
One-pot $Bi_{24}O_{31}Br_{10}$	**2.64**	**~470**	**99**
CdS-$Bi_{24}O_{31}Br_{10}$	**2.6**	**473**	**100**
$Bi_{24}O_{31}Br_{10}$ nanoflakes	**2.51**	**~494**	**101**
BiOBr/$Bi_{24}O_{31}Br_{10}$/TiO_2	**2.64**	**470**	**102**
BOB-S	**2.3**	**~539**	**103**
BOB-M	**2.33**	**~532**	**103**
BOB-L	**2.35**	**~528**	**103**
BUC-21/$Bi_{24}O_{31}Br_{10}$	**2.65**	**~468**	**104**
$Bi_{24}O_{31}Br_{10}$-nanobelts	**2.45**	**~506**	**105**
$Bi_{24}O_{31}Br_{10}$-nanosheets	**2.53**	**~490**	**105**
$Bi_{24}O_{31}Br_{10}$/$SrTiO_3$	**2.79**	**465**	**106**
$Bi_4O_5Br_2$/$Bi_{24}O_{31}Br_{10}$/Bi_2SiO_5	**2.79**	**444**	**107**
$Bi_{24}O_{31}Br_{10}$ PSQDs	**2.83**	**~438**	**108**
VBi-$Bi_{24}O_{31}Br_{10}$	**2.87**	**~432**	**109**
$Bi_{24}O_{31}Cl_xBr_{10-x}(Bi_{24}O_{31}Br_{10})$	**2.68**	**~463**	**110**
$Bi_{24}O_{31}Br_{10}$-pH	**2.4**	**500**	**111**

Table S5 Band gap and UV-vis absorption of Bi_3O_4Br.

Sample	Gap(eV)	UV-vis(nm)	Ref
$AgBr/Bi_3O_4Br$	2.55	~486	112
$CQD\text{-}Bi_3O_4Br$	2.68	463	113
$Bi_3O_4Br/BiOCl$	2.42	512	114
AgI/Bi_3O_4Br	2.4	550	115
bulk Bi_3O_4Br	2.42	~512	116
$Bi_3O_4Br\text{-}Bi_{24}O_{31}Br_{10}$	2.25	600	95
$Bi_3O_4Br\text{-}BiOBr$	2.4	467	51
Bi_3O_4Br nanoplates	2.64	470	117
$Bi_3O_4Br/CuBi_2O_4$	2.83	~438	118
$\alpha\text{-}Bi_2O_3/Bi_3O_4Br$	2.65	~468	119
$Bi_3O_4Br/NH_2\text{-}MIL\text{-}125(Ti)$	2.5	476	120
$C\text{-}Bi_3O_4Br$	2.31	537	121
Bi_3O_4Br/Bi_2O_3	2.58	~481	122
$C\text{-}Bi_3O_4Br\text{-}1$	2.5	538	123

Table S6 Band gap and UV-vis absorption of Bi_5O_7Br.

Sample	Gap(eV)	UV-vis(nm)	Ref
$Bi\text{-}Bi_5O_7Br$	2.38	521	124
$Bi_5O_7Br/BiOBr$	2.38	507	52
Bi_2MoO_6/Bi_5O_7Br	2.31	~537	125

Bi_5O_7Br	**3.13**	**396**	**126**
5-Bi_5O_7Br-NT	**2.89**	**~429**	**127**
$Bi_5O_7Br_{0.5}I_{0.5}$(Bi_5O_7I, Bi_5O_7Br)	**2.21**	**441**	**128**
Bi_5O_7Br/NiFe-LDH	**2.65**	**520**	**129**
Bi_5O_7Br nanowires	**2.98**	**~416**	**130**
Ag/Bi_5O_7Br	**2.22**	**517**	**131**
BiOBr@$Bi_4O_5Br_2$@Bi_5O_7Br	**2.64**	**470**	**53**

The formation energy is calculated using the following formula:

$$E_{formation}=E_{compound}-\sum n_i\mu_i$$

where $E_{compound}$ is the total energy of the compound, μ_i is the chemical potential of the constituent element, and n_i is the number of elements in the compound. The chemical potential μ_i is the energy obtained from the element's monomers or its stable phase, depending on the conditions of the calculation.

Table S7 The formation energy of $Bi_xO_yBr_z$.

	Number of atoms	**Formation Energy（eV / atom）**	**Method**
BiOBr	**6**	**-1.55**	**Meta-GGA**

Bi_2OBr_2	**20**	**-0.46**	**Meta-GGA**
Bi_3O_4Br	**32**	**-1.53**	**Meta-GGA**
$Bi_4O_5Br_2$	**44**	**-1.55**	**Meta-GGA**
Bi_5O_7Br	**104**	**-1.53**	**Meta-GGA**
$Bi_{12}O_{16}Br_5$	**66**	**-1.51**	**Meta-GGA**
$Bi_{24}O_{31}Br_{10}$	**65**	**-1.51**	**Meta-GGA**

Reference

1. Zhao, L. J.; Zhang, X. C.; Fan, C. M.; Liang, Z. H.; Han, P. D., First-principles study on the structural, electronic and optical properties of BiOX (X=Cl, Br, I) crystals. *Physica B: Condensed Matter* **2012,** *407* (17), 3364-3370.

2. Aurivillius, B., CRYSTAL-STRUCTURE OF NDBI5O8CL2 SINGLE-CRYSTAL INVESTIGATIONS ON BI3O4BR AND BI12O17CL2-(RE,BI) 3O4+XX AND BI3O4BR CRYSTAL-STRUCTURES-X=CL,BR,SE.RE=CE,ND. *Chemica Scripta* **1984,** *24* (3), 125-129.

3. Keller, E.; Ketterer, J.; Krämer, V., Crystal structure and twinning of $Bi_4O_5Br_2$. *Zeitschrift fur Kristallographie* **2001,** *216* (11), 595-599.

4. Keller, E.; Krämer, V., Bi_5O_7Br and its structural relation to α-Bi_5O_7I. *Acta Crystallographica Section C: Structural Chemistry* **2007,** *63*, I109-I111.

5. Shang, J.; Hao, W. C.; Lv, X. J.; Wang, T. M.; Wang, X. L.; Du, Y.; Dou, S. X.; Xie, T. F.; Wang, D. J.; Wang, J. O., Bismuth Oxybromide with Reasonable Photocatalytic Reduction Activity under Visible Light. *Acs Catalysis* **2014,** *4* (3), 954-961.

6. Yin, H.; Chen, X.; Hou, R.; Zhu, H.; Li, S.; Huo, Y.; Li, H., Ag/BiOBr film in a rotating-disk reactor containing long-afterglow phosphor for round-the-clock photocatalysis. *ACS Applied Materials & Interfaces* **2015,** *7* (36), 20076-20082.

7. Maisang, W.; Promnopas, S.; Kaowphong, S.; Narksitipan, S.; Thongtem, S.; Wannapop, S.; Phuruangrat, A.; Thongtem, T., Microwave-assisted hydrothermal synthesis of BiOBr/BiOCl flowerlike composites used for photocatalysis. *Research on Chemical Intermediates* **2020,** *46*, 2117-2135.

8. Li, J.; Sun, S.; Qian, C.; He, L.; Chen, K. K.; Zhang, T.; Chen, Z.; Ye, M., The role of adsorption in photocatalytic degradation of ibuprofen under visible light irradiation by BiOBr microspheres. *Chemical Engineering Journal* **2016,** *297*, 139-147.

9. Yang, Q.; Li, X.; Tian, Q.; Pan, A.; Liu, X.; Yin, H.; Shi, Y.; Fang, G., Synergistic effect of adsorption and photocatalysis of BiOBr/lignin-biochar composites with oxygen vacancies under visible light irradiation. *Journal of Industrial and Engineering Chemistry* **2023,** *117*, 117-129.

10. Shi, X., PingquanWang, LiBai, YangXie, HaiquanZhou, YingWang, Jin AnLi, ZhongjunQu, LingboShi, MingjiYe, Liqun, Few Layered BiOBr with Expanded Interlayer Spacing and Oxygen Vacancies for Efficient Decomposition of Real Oil Field Produced Wastewater. *ACS Sustainable Chemistry & Engineering* **2018,** *6* (11).

11. Zhao, C.; Liang, Y.; Li, W.; Tian, Y.; Chen, X.; Yin, D.; Zhang, Q., BiOBr/BiOCl/carbon quantum dot microspheres with superior visible light-driven photocatalysis. *RSC advances* **2017,** *7* (83), 52614-52620.

12. Deng, W.; Pan, F.; Batchelor, B.; Jung, B.; Zhang, P.; Abdel-Wahab, A.; Zhou, H.; Li, Y., Mesoporous TiO_2–BiOBr microspheres with tailorable adsorption capacities for photodegradation of organic water pollutants: probing adsorption–photocatalysis synergy by combining experiments and kinetic modeling. *Environmental Science: Water Research & Technology* **2019,** *5* (4), 769-781.

13. Qiu, J.; Wu, M.; Yu, L.; Li, J.; Di, J.; Zhang, S.; Luo, Z.; Zhang, S.; Li, Z.; Wu, Z., Vanadate-Rich BiOBr/Bi Nanosheets for Effective Adsorption and Visible-Light-Driven Photodegradation of Rhodamine B. *Journal of Nanoscience and Nanotechnology* **2020,** *20* (4), 2267-2276.

14. Wu, D.; Tan, H.; Wu, C., The novel 2D-2D pn heterojunction BiOBr/$Bi_{12}O_{15}Cl_6$ composites with

enhanced visible light photocatalytic activity. *Journal of Optoelectronics and Advanced Materials* **2018,** *20* (July-August 2018), 445-450.

15. Guo, Y.; Wen, H.; Zhong, T.; Huang, H.; Lin, Z., Core-shell-like BiOBr@BiOBr homojunction for enhanced photocatalysis. *Colloids and Surfaces A: Physicochemical and Engineering Aspects* **2022,** *644*, 128829.

16. Song, W.; Zhao, J.; Xie, X.; Liu, W.; Liu, S.; Chang, H.; Wang, C., Novel BiOBr by compositing low-cost biochar for efficient ciprofloxacin removal: the synergy of adsorption and photocatalysis on the degradation kinetics and mechanism insight. *RSC advances* **2021,** *11* (25), 15369-15379.

17. Zhang, W.; Sun, Y.; Li, J.; Cen, W.; Cui, Z.; Huang, H.; Dong, F., Visible-light-induced charge transfer pathway and photocatalysis mechanism on Bi semimetal@defective BiOBr hierarchical microspheres. *Journal of catalysis* **2018,** *357*, 41-50.

18. Qu, S.; Xiong, Y.; Zhang, J., Graphene oxide and carbon nanodots co-modified BiOBr nanocomposites with enhanced photocatalytic 4-chlorophenol degradation and mechanism insight. *Journal of colloid and interface science* **2018,** *527*, 78.

19. Meng, L.; Qu, Y.; Jing, L., Recent advances in BiOBr-based photocatalysts for environmental remediation. *Chinese Chemical Letters* **2021,** *32* (11), 3265-3276.

20. Lyu, J.; Li, Z.; Ge, M., Novel Bi/BiOBr/AgBr composite microspheres: Ion exchange synthesis and photocatalytic performance. *Solid State Sciences* **2018,** *80*, 101-109.

21. Gupta, G.; Kaur, A.; Sinha, A.; Kansal, S. K., Photocatalytic degradation of levofloxacin in aqueous phase using Ag/AgBr/BiOBr microplates under visible light. *Materials Research Bulletin* **2017,** *88*, 148-155.

22. Lyu, J.; Hu, Z.; Li, Z.; Ge, M., Removal of tetracycline by BiOBr microspheres with oxygen vacancies: Combination of adsorption and photocatalysis. *Journal of Physics and Chemistry of Solids* **2019,** *129*, 61-70.

23. Li, Z.; Zhang, H.; Wang, L.; Meng, X.; Shi, J.; Qi, C.; Zhang, Z.; Feng, L.; Li, C., 2D/2D BiOBr/Ti_3C_2 heterojunction with dual applications in both water detoxification and water splitting. *Journal of Photochemistry and Photobiology A: Chemistry* **2020,** *386*, 112099.

24. Xu, G.; Li, M.; Wang, Y.; Zheng, N.; Yang, L.; Yu, H.; Yu, Y., A novel Ag-BiOBr-rGO photocatalyst for enhanced ketoprofen degradation: Kinetics and mechanisms. *Science of the total environment* **2019,** *678*, 173-180.

25. Liu, D.; Xie, J.; Xia, Y., Improved photocatalytic activity of MWCNT/BiOBr composite synthesized via interfacial covalent bonding linkage. *Chemical Physics Letters* **2019,** *729*, 42-48.

26. Maisang, W.; Phuruangrat, A.; Randorn, C.; Kungwankunakorn, S.; Thongtem, S.; Wiranwetchayan, O.; Wannapop, S.; Choopun, S.; Kaowphong, S.; Thongtem, T., Enhanced photocatalytic performance of visible-light-driven BiOBr/$BiPO_4$ composites. *Materials Science in Semiconductor Processing* **2018,** *75*, 319-326.

27. Wang, Y.; He, J.; Zhu, Y.; Zhang, H.; Yang, C.; Wang, K.; Wu, S.-c.; Chueh, Y.-L.; Jiang, W., Hierarchical Bi-doped BiOBr microspheres assembled from nanosheets with (001) facet exposed via crystal facet engineering toward highly efficient visible light photocatalysis. *Applied Surface Science* **2020,** *514*, 145927.

28. Lei, H.; Zhang, H.; Zou, Y.; Dong, X.; Jia, Y.; Wang, F., Synergetic photocatalysis/piezocatalysis of bismuth oxybromide for degradation of organic pollutants. *Journal of Alloys and Compounds* **2019,** *809*, 151840.

29. Dong, Y.; Feng, C.; Zhang, J.; Jiang, P.; Wang, G.; Wu, X.; Miao, H., A New p-Metal-n Structure

AgBr-Ag-BiOBr with Superior Visible-Light-Responsive Catalytic Performance. *Chemistry–An Asian Journal* **2015,** *10* (3), 687-693.

30. Wang, B.; Di, J.; Xia, J.; Xu, L.; Xu, H.; Zhang, Q.; Chen, Z.; Li, H., Graphene-like BN/BiOBr composite: synthesis via a reactable ionic liquid and enhanced visible light photocatalytic performance. *Materials Technology* **2016,** *31* (8), 463-470.

31. Feng, H.; Xu, Z.; Wang, L.; Yu, Y.; Mitchell, D.; Cui, D.; Xu, X.; Shi, J.; Sannomiya, T.; Du, Y., Modulation of photocatalytic properties by strain in 2D BiOBr nanosheets. *ACS applied materials & interfaces* **2015,** *7* (50), 27592-27596.

32. Zhao, C.; Li, W.; Liang, Y.; Tian, Y.; Zhang, Q., Synthesis of BiOBr/carbon quantum dots microspheres with enhanced photoactivity and photostability under visible light irradiation. *Applied Catalysis A: General* **2016,** *527*, 127-136.

33. Shi, M.; Li, G.; Li, J.; Jin, X.; Tao, X.; Zeng, B.; Pidko, E. A.; Li, R.; Li, C., Intrinsic facet-dependent reactivity of well-defined BiOBr nanosheets on photocatalytic water splitting. *Angewandte Chemie* **2020,** *132* (16), 6652-6657.

34. Wu, X.; Zhang, K.; Zhang, G.; Yin, S., Facile preparation of BiOX (X= Cl, Br, I) nanoparticles and up-conversion phosphors/BiOBr composites for efficient degradation of NO gas: Oxygen vacancy effect and near infrared light responsive mechanism. *Chemical Engineering Journal* **2017,** *325*, 59-70.

35. Feng, S.; Yan, Z.; Ni, Q.; Zhang, Y., In-situ synthesis of 3D BiOBr/UiO-66-NH_2 heterojunction nanocomposite and its excellent photocatalytic degradation of rhodamine B dye. *Frontiers in Environmental Science* **2022,** *10*, 994152.

36. Xiao, Y.; Maimaitizi, H.; Okitsu, K.; Tursun, Y.; Abulizi, A., Sonochemical Fabrication of s-Scheme Hierarchical CdS/BiOBr Heterojunction Photocatalyst with High Performance for Carbon Dioxide Reduction. *Particle & Particle Systems Characterization* **2022,** *39* (4), 2200019.

37. Liu, Y.; He, J.; Qi, Y.; Wang, Y.; Long, F.; Wang, M., Preparation of flower-like BiOBr/Bi_2WO_6 Z-scheme heterojunction through an ion exchange process with enhanced photocatalytic activity. *Materials Science in Semiconductor Processing* **2022,** *137*, 106195.

38. Gao, D.; Dong, Z.; Feng, W.; Li, Z.; Wu, H.; Wu, Y.; Wei, Q.; Meng, C.; Wu, Y.; Wang, Y., Dipole Moment and Built-In Polarization Electric Field Induced by Oxygen Vacancies in BiOX for Boosting Piezoelectric–Photocatalytic Removal of Uranium (VI). *Inorganic Chemistry* **2024,** *63* (13), 5931-5944.

39. Xie, Z.; Hu, M.; Qiu, X.; Guo, X.; Chen, P.; Jiang, H.; Luo, X.; Fominski, V., A S-scheme heterojunction of MIL-125(Ti)/BiOBr for remediation of organic and inorganic pollutants coexistent real water: Application and mechanism investigation. *Journal of Environmental Chemical Engineering* **2024,** *12* (3), 112567.

40. Andrade, A. O.; da Silveira Lacerda, L. H.; Júnior, M. L.; Sharma, S. K.; da Costa, M. M.; Alves, O. C.; Santos, E. C.; dos Santos, C.; de Menezes, A.; San-Miguel, M. A., Enhanced photocatalytic activity of BiOBr/$ZnWO_4$ heterojunction: A combined experimental and DFT-based theoretical approach. *Optical Materials* **2023,** *138*, 113701.

41. Hu, Y.; Hu, X.; Xue, L.; Cui, B.; Du, Y., Preparation of $CaCO_3$ mediated BiOBr that rich (1 1 0) facet and research of the photocatalytic properties. *Applied Surface Science* **2022,** *598*, 153800.

42. Tong, Y.; Ma, Z.; He, Y., Boron nitride nanosheets modified BiOBr photocatalysts for promoting photocatalytic removal of tetracycline under visible light irradiation. *Optical Materials* **2024,** *150*, 115248.

43. Qu, Y.; Chen, Z.; Duan, Y.; Liu, L., H_2O_2 assisted photocatalysis over Fe-MOF modified BiOBr for degradation of RhB. *Journal of Chemical Technology & Biotechnology* **2022,** *97* (10), 2881-2888.

44. Long, Z.; Zhang, G.; Du, H.; Zhu, J.; Li, J., Preparation and application of BiOBr-Bi_2S_3 heterojunctions for efficient photocatalytic removal of Cr (VI). *Journal of Hazardous Materials* **2021,** *407*, 124394.

45. Lv, X.; Yan, D. Y.; Lam, F. L.-Y.; Ng, Y. H.; Yin, S.; An, A. K., Solvothermal synthesis of copper-doped BiOBr microflowers with enhanced adsorption and visible-light driven photocatalytic degradation of norfloxacin. *Chemical Engineering Journal* **2020,** *401*, 126012.

46. Di, J.; Xia, J.; Ji, M.; Wang, B.; Yin, S.; Zhang, Q.; Chen, Z.; Li, H., Advanced photocatalytic performance of graphene-like BN modified BiOBr flower-like materials for the removal of pollutants and mechanism insight. *Applied Catalysis B: Environmental* **2016,** *183*, 254-262.

47. Zhang, M.; Lai, C.; Li, B.; Huang, D.; Zeng, G.; Xu, P.; Qin, L.; Liu, S.; Liu, X.; Yi, H., Rational design 2D/2D BiOBr/CDs/g-C_3N_4 Z-scheme heterojunction photocatalyst with carbon dots as solid-state electron mediators for enhanced visible and NIR photocatalytic activity: kinetics, intermediates, and mechanism insight. *Journal of catalysis* **2019,** *369*, 469-481.

48. Ao, Y.; Wang, K.; Wang, P.; Wang, C.; Hou, J., Synthesis of novel 2D-2D pn heterojunction BiOBr/$La_2Ti_2O_7$ composite photocatalyst with enhanced photocatalytic performance under both UV and visible light irradiation. *Applied Catalysis B: Environmental* **2016,** *194*, 157-168.

49. Kumar, A.; Sharma, S. K.; Sharma, G.; Ala'a, H.; Naushad, M.; Ghfar, A. A.; Stadler, F. J., Wide spectral degradation of Norfloxacin by Ag@BiPO4/BiOBr/$BiFeO_3$ nano-assembly: elucidating the photocatalytic mechanism under different light sources. *Journal of hazardous materials* **2019,** *364*, 429-440.

50. Liu, C.; Mao, S.; Shi, M.; Wang, F.; Xia, M.; Chen, Q.; Ju, X., Peroxymonosulfate activation through 2D/2D Z-scheme CoAl-LDH/BiOBr photocatalyst under visible light for ciprofloxacin degradation. *Journal of Hazardous materials* **2021,** *420*, 126613.

51. Wang, J.; Yu, Y.; Zhang, L., Highly efficient photocatalytic removal of sodium pentachlorophenate with Bi_3O_4Br under visible light. *Applied Catalysis B: Environmental* **2013,** *136*, 112-121.

52. Zhang, L.; Yue, X.; Liu, J.; Feng, J.; Zhang, X.; Zhang, C.; Li, R.; Fan, C., Facile synthesis of Bi_5O_7Br/BiOBr 2D/3D heterojunction as efficient visible-light-driven photocatalyst for pharmaceutical organic degradation. *Separation and Purification Technology* **2020,** *231*, 115917.

53. Wang, Y.; He, H.; Wang, Y.; Xie, M.; Jing, F.; Yin, X.; Hu, F.; Mi, Y., Surface defect and lattice engineering of Bi_5O_7Br ultrathin nanosheets for efficient photocatalysis. *Nano Research* **2023,** *16* (1), 248-255.

54. Cao, W.; Chen, C.; Zhou, H.; Yang, J.; Jiang, C.; Wang, Y., In situ preparation of 3D flower sphere $Bi_4O_5Br_2$/$Bi_{24}O_{31}Br_{10}$ heterojunctions by calcination for enhanced antibiotic degradation. *Colloids and Surfaces A: Physicochemical and Engineering Aspects* **2021,** *629*, 127373.

55. Bai, Y.; Yang, P.; Wang, L.; Yang, B.; Xie, H.; Zhou, Y.; Ye, L., Ultrathin $Bi_4O_5Br_2$ nanosheets for selective photocatalytic CO_2 conversion into CO. *Chemical Engineering Journal* **2019,** *360*, 473-482.

56. Zhang, Y.; Pan, H.; Zhang, F., Solvothermal synthesis of CDs/$Bi_4O_5Br_2$ nanocomposites with improved visible-light photocatalytic ciprofloxacin (CIP) decontamination. *Materials Letters* **2019,** *251*, 114-117.

57. Ding, S.; Han, M.; Dai, Y.; Yang, S.; Mao, D.; He, H.; Sun, C., Synthesis of Ag/AgBr/$Bi_4O_5Br_2$ plasmonic heterojunction photocatalysts: elevated visible-light photocatalytic performance and Z-scheme mechanism. *ChemCatChem* **2019,** *11* (15), 3490-3504.

58. Xiao, X.; Lu, M.; Nan, J.; Zuo, X.; Zhang, W.; Liu, S.; Wang, S., Rapid microwave synthesis of I-doped $Bi_4O_5Br_2$ with significantly enhanced visible-light photocatalysis for degradation of multiple parabens. *Applied Catalysis B: Environmental* **2017**.

59. Mao, X.; Xie, F.; Li, M., Facile hydrolysis synthesis of novel $Bi_4O_5Br_2$ photocatalyst with enhanced visible light photocatalytic activity for the degradation of resorcinol. *Materials Letters* **2016,** *166*, 296-299.

60. Cao, W.; Jiang, C.; Chen, C.; Zhou, H.; Wang, Y., A novel Z-scheme CdS/$Bi_4O_5Br_2$ heterostructure with mechanism analysis: Enhanced photocatalytic performance. *Journal of Alloys and Compounds* **2021,** *861*, 158554.

61. Yi, F.; Ma, J.; Lin, C.; Wang, L.; Zhang, H.; Qian, Y.; Zhang, K., Insights into the enhanced adsorption/photocatalysis mechanism of a $Bi_4O_5Br_2$/g-C_3N_4 nanosheet. *Journal of Alloys and Compounds* **2020,** *821*, 153557.

62. Chang, F.; Yang, C.; Wang, J.; Lei, B.; Li, S.; Kim, H., Enhanced photocatalytic conversion of NOx with satisfactory selectivity of 3D-2D $Bi_4O_5Br_2$-GO hierarchical structures via a facile microwave-assisted preparation. *Separation and Purification Technology* **2021,** *266*, 118237.

63. Mi, Y.; Li, H.; Zhang, Y.; Hou, W., Synthesis of belt-like bismuth-rich bismuth oxybromide hierarchical nanostructures with high photocatalytic activities. *Journal of colloid and interface science* **2019,** *534*, 301-311.

64. Wu, Z.; Shen, J.; Ma, N.; Li, Z.; Wu, M.; Xu, D.; Zhang, S.; Feng, W.; Zhu, Y., $Bi_4O_5Br_2$ nanosheets with vertical aligned facets for efficient visible-light-driven photodegradation of BPA. *Applied Catalysis B: Environmental* **2021,** *286*, 119937.

65. Zhao, X.; You, Y.; Huang, S.; Wu, Y.; Ma, Y.; Zhang, G.; Zhang, Z., Z-scheme photocatalytic production of hydrogen peroxide over $Bi_4O_5Br_2$/g-C_3N_4 heterostructure under visible light. *Applied Catalysis B: Environmental* **2020,** *278*, 119251.

66. Liu, J.; Li, R.; Zu, X.; Zhang, X.; Wang, Y.; Wang, Y.; Fan, C., Photocatalytic conversion of nitrogen to ammonia with water on triphase interfaces of hydrophilic-hydrophobic composite $Bi_4O_5Br_2$/ZIF-8. *Chemical Engineering Journal* **2019,** *371*, 796-803.

67. Qi, Y.; Chang, F.; Wang, Y.; Zhang, T.; Liu, X.; Chen, S., $Bi_4O_5Br_2$-based binary composites: Facile fabrication, characterization, and enhanced photocatalytic performance over NO removal. *Materials Science in Semiconductor Processing* **2021,** *129*, 105788.

68. Mao, D.; Ding, S.; Meng, L.; Dai, Y.; Sun, C.; Yang, S.; He, H., One-pot microemulsion-mediated synthesis of Bi-rich $Bi_4O_5Br_2$ with controllable morphologies and excellent visible-light photocatalytic removal of pollutants. *Applied Catalysis B: Environmental* **2017,** *207*, 153-165.

69. Di, J.; Xia, J.; Ji, M.; Yin, S.; Li, H.; Xu, H.; Zhang, Q.; Li, H., Controllable synthesis of $Bi_4O_5Br_2$ ultrathin nanosheets for photocatalytic removal of ciprofloxacin and mechanism insight. *Journal of Materials Chemistry A* **2015,** *3* (29), 15108-15118.

70. Xia, J.; Ge, Y.; Di, J.; Xu, L.; Yin, S.; Chen, Z.; Liu, P.; Li, H., Ionic liquid-assisted strategy for bismuth-rich bismuth oxybromides nanosheets with superior visible light-driven photocatalytic removal of bisphenol-A. *Journal of colloid and interface science* **2016,** *473*, 112-119.

71. Wang, C.; Sun, X.; Zhang, M.; Wang, Y.; Tan, Z.; Li, J.; Xi, B., Ultrasound-assisted room-temperature in situ precipitation synthesis of BC doped $Bi_4O_5Br_2$ for enhanced photocatalytic activity in pollutants degradation under visible light. *Journal of Alloys and Compounds* **2022,** *889*, 161609.

72. Wang, Y.; Xiao, X.; Ding, T.; Lu, M., Mixed 1T-2H phase $MoSe_2$ as interfacial charge-transfer-bridge to boosting photocatalytic activity of dual Z-scheme AgI/1T-2H $MoSe_2$/$Bi_4O_5Br_2$ heterojunction. *Journal of Alloys and Compounds* **2021,** *875*, 160092.

73. Sedaghati, N.; Habibi-Yangjeh, A.; Asadzadeh-Khaneghah, S.; Ghosh, S., Photocatalytic performance of oxygen vacancy rich-TiO_2 combined with $Bi_4O_5Br_2$ nanoparticles on degradation of

several water pollutants. *Advanced Powder Technology* **2021,** *32* (2), 304-316.

74. Li, R.; Liu, J.; Zhang, X.; Wang, Y.; Wang, Y.; Zhang, C.; Zhang, X.; Fan, C., Iodide-modified $Bi_4O_5Br_2$ photocatalyst with tunable conduction band position for efficient visible-light decontamination of pollutants. *Chemical Engineering Journal* **2018,** *339*, 42-50.

75. Li, P.; Cao, W.; Zhu, Y.; Teng, Q.; Peng, L.; Jiang, C.; Feng, C.; Wang, Y., NaOH-induced formation of 3D flower-sphere BiOBr/$Bi_4O_5Br_2$ with proper-oxygen vacancies via in-situ self-template phase transformation method for antibiotic photodegradation. *Science of the total environment* **2020,** *715*, 136809.

76. Chang, F.; Li, S.; Shi, Z.; Qi, Y.; Liu, D.-g.; Liu, X.; Chen, S., Boosted photocatalytic NO removal performance by S-scheme hierarchical composites WO_3/$Bi_4O_5Br_2$ prepared through a facile ball-milling protocol. *Separation and Purification Technology* **2021,** *278*, 119662.

77. Zhao, Y.; Cao, X.; Zheng, R.; Zhang, H.; Liang, X., NaOH and temperature-induced formation of Bi-based $Bi_xO_yBr_z$ photocatalyst for phenol degradation. *Materials Letters* **2023,** *353*, 135229.

78. Cao, W.; Wang, M.; Yang, J.; Han, B.; Zhu, X.; Wang, Y., 3D flower sphere Bi_2S_3/$Bi_4O_5Br_2$ heterojunction: Alleviating photocorrosion and enhanced photocatalytic performance. *Journal of Solid State Chemistry* **2022,** *312*, 123172.

79. He, S.; Yang, Y.; Fan, Y.; Ding, C.; Wang, H., Preparation of $Bi_4O_5Br_2$/graphene and photocatalytic performance study. *Ferroelectrics* **2022,** *595* (1), 156-162.

80. Jin, X.; Cao, J.; Wang, H.; Lv, C.; Xie, H.; Su, F.; Li, X.; Sun, R.; Shi, S.; Dang, M., Realizing improved CO_2 photoreduction in Z-scheme $Bi_4O_5Br_2$/AgBr heterostructure. *Applied Surface Science* **2022,** *598*, 153758.

81. Dong, X.; Xu, L.; Ma, J.; Li, Y.; Yin, Z.; Chen, D.; Wang, Q.; Han, J.; Qiu, J.; Yang, Z., Enhanced interfacial charge transfer and photothermal effect via in-situ construction of atom co-sharing Bi plasmonic/$Bi_4O_5Br_2$ nanosheet heterojunction towards improved full-spectrum photocatalysis. *Chemical Engineering Journal* **2023,** *459*, 141557.

82. Zhang, K.; Chen, H.; Pei, W.; Dai, H.; Li, J.; Zhu, Y., Enhanced photocatalytic performance of $Bi_4O_5Br_2$ with three-dimensionally ordered macroporous structure for phenol removal. *Nano Research* **2023,** *16* (7), 8871-8881.

83. Sun, J.; Li, X.; Li, J.; Mu, M.; Yin, X., Fabrication of $Bi_4O_5Br_2$-decorated rod-like MOF-derived MoS_2 hierarchical heterostructures for boosting photocatalytic CO_2 reduction. *Colloids and Surfaces A: Physicochemical and Engineering Aspects* **2022,** *653*, 129940.

84. Chang, F.; Wang, X.; Li, S.; Chen, H.; Wang, Y.; Liu, D.-g., Strengthened photocatalytic removal of bisphenol A under visible light by magnetic ternary heterojunctions $Bi_4O_5Br_2$/$Bi_4O_5I_2$/Fe_3O_4. *Journal of Alloys and Compounds* **2022,** *908*, 164644.

85. Zhao, L.; Fang, W.; Meng, X.; Wang, L.; Bai, H.; Li, C., In-situ synthesis of metal Bi to improve the stability of oxygen vacancies and enhance the photocatalytic activity of $Bi_4O_5Br_2$ in H_2 evolution. *Journal of Alloys and Compounds* **2022,** *910*, 164883.

86. Wang, H.; Wang, Y.; Xu, L.; Zhang, M.; Wu, X.; Hejing, L., Novel $Bi_4O_5Br_2$/$Mn_xZn_{1-x}Fe_2O_4$ magnetic composite with an enhanced photodegradation activity and excellent recyclability. *Ceramics International* **2022,** *48* (15), 21988-21995.

87. Vadivel, S.; Fujii, M.; Rajendran, S., Novel S-scheme 2D/2D $Bi_4O_5Br_2$ nanoplatelets/g-C_3N_5 heterojunctions with enhanced photocatalytic activity towards organic pollutants removal. *Environmental Research* **2022,** *213*, 113736.

88. Zhang, F.; Peng, Y.; Yang, X.; Li, Z.; Zhang, Y., Enhanced Photo-Assisted Fenton Degradation of

Antibiotics over Iron-Doped Bi-Rich Bismuth Oxybromide Photocatalyst. *Nanomaterials* **2022,** *13* (1), 188.

89. Li, L.; Liu, G.; Dong, J.; Zhang, Y.; Cao, S.; Wang, K.; Wang, B.; She, Y.; Xia, J.; Li, H., In Situ Construction of CuTCPP/$Bi_4O_5Br_2$ Hybrids for Improved Photocatalytic CO_2 and Cr(VI) Reduction. *Inorganic Chemistry* **2024**.

90. Mao, D.; Hu, Y.; Yang, S.; Liang, J.; He, H.; Yang, S.; Xu, Z.; Sun, C.; Zheng, S.; Jiang, Z., Oxygen-vacancy-induced charge localization and atomic site activation in ultrathin $Bi_4O_5Br_2$ nanotubes for boosted CO_2 photoreduction. *Chemical Engineering Journal* **2023,** *452*, 139304.

91. Dong, X.; Yin, Z.; Xu, L.; Ma, J.; Cao, H.; Li, Y.; Wang, Q.; Han, J.; Qiu, J.; Yang, Z., Effective BPA degradation via atom-sharing Bi/$Bi_4O_5Br_2$: Yb^{3+}, Tm^{3+} plasma heterojunctions with enhanced charge transfer and light absorption. *Ceramics International* **2024,** *50* (2), 4083-4091.

92. Liu, H.; Ding, H.; Zahid, A. H.; Han, Q., CTAB-assisted construction of 3D flower-sphere S-scheme $Bi_{12}O_{17}Br_2$/$Bi_4O_5Br_2$ heterojunction with enhanced visible-light photocatalytic performance. *Colloids and Surfaces A: Physicochemical and Engineering Aspects* **2022,** *654*, 130029.

93. Chang, F.; Zhao, S.; Lei, Y.; Peng, S.; Liu, D.-g.; Kong, Y., Ball-milling fabrication of np heterojunctions $Bi_4O_5Br_2$/α-MnS with strengthened photocatalytic removal of bisphenol A in a Z-Scheme model. *Separation and Purification Technology* **2023,** *304*, 122324.

94. Huang, F.; Humayun, M.; Li, G.; Fan, T.-T.; Wang, W.-L.; Cao, Y.-L.; Nikiforov, A.; Wang, C.-D.; Wang, J., Z-scheme $Bi_4O_5Br_2$/NH_2-MIL-125(Ti) heterojunctions enable exceptional visible photocatalytic degradation of organic pollutant. *Rare Metals* **2024**, 1-12.

95. Li, R.; Feng, J.; Zhang, X.; Xie, F.; Liu, J.; Zhang, C.; Wang, Y.; Yue, X.; Fan, C., In situ reorganization of Bi3O4Br nanosheet on the $Bi_{24}O_{31}Br_{10}$ ribbon structure for superior visible-light photocatalytic capability. *Separation and Purification Technology* **2020,** *247*, 117007.

96. Zeng, Q.; Xie, W.; Chen, Z.; Wang, X.; Akinoglu, E. M.; Zhou, G.; Shui, L., Influence of the facets of $Bi_{24}O_{31}Br_{10}$ nanobelts and nanosheets on their photocatalytic properties. *Catalysts* **2020,** *10* (2), 257.

97. Zheng, H.; Chen, G.; Zhang, A.; Tan, Z.; Wang, R.; Wang, H.; Mei, Y.; Zhang, X.; Ran, J., Enhanced photocatalytic activity of $Bi_{24}O_{31}Br_{10}$ microsheets constructing heterojunction with AgI for Hg0 removal. *Separation and Purification Technology* **2021,** *262*, 118296.

98. Dai, Y.; Ren, P.; Li, Y.; Lv, D.; Shen, Y.; Li, Y.; Niemantsverdriet, H.; Besenbacher, F.; Xiang, H.; Hao, W., Solid Base $Bi_{24}O_{31}Br_{10}$(OH)δ with Active Lattice Oxygen for the Efficient Photo-Oxidation of Primary Alcohols to Aldehydes. *Angewandte Chemie International Edition* **2019,** *58* (19), 6265-6270.

99. Liu, Z.; Ran, H.; Niu, J.; Feng, P.; Zhu, Y., One-pot synthesis of Bismuth Oxyhalide/Oxygen-rich bismuth oxyhalide Heterojunction and its photocatalytic activity. *Journal of colloid and interface science* **2014,** *431*, 187-193.

100. Mou, Q.; Guo, Z.; Chai, Y.; Liu, B.; Liu, C., Visible-light assisted photoreduction of CO_2 using CdS-decorated $Bi_{24}O_{31}Br_{10}$. *Materials Science in Semiconductor Processing* **2021,** *134*, 106011.

101. Xiao, X.; Hu, R.; Liu, C.; Xing, C.; Zuo, X.; Nan, J.; Wang, L., Facile microwave synthesis of novel hierarchical $Bi_{24}O_{31}Br_{10}$ nanoflakes with excellent visible light photocatalytic performance for the degradation of tetracycline hydrochloride. *Chemical Engineering Journal* **2013,** *225*, 790-797.

102. Zhu, S.-R.; Wu, M.-K.; Zhao, W.-N.; Yi, F.-Y.; Tao, K.; Han, L., Fabrication of heterostructured BiOBr/$Bi_{24}O_{31}Br_{10}$/TiO_2 photocatalyst by pyrolysis of MOF composite for dye degradation. *Journal of Solid State Chemistry* **2017,** *255*, 17-26.

103. Wang, C.-Y.; Zhang, X.; Qiu, H.-B.; Huang, G.-X.; Yu, H.-Q., $Bi_{24}O_{31}Br_{10}$ nanosheets with controllable thickness for visible–light–driven catalytic degradation of tetracycline hydrochloride. *Applied Catalysis*

B: Environmental **2017,** *205*, 615-623.

104. Zhao, C.; Wang, Z.; Li, X.; Yi, X.; Chu, H.; Chen, X.; Wang, C.-C., Facile fabrication of BUC-21/$Bi_{24}O3_1Br_{10}$ composites for enhanced photocatalytic Cr(VI) reduction under white light. *Chemical Engineering Journal* **2020,** *389*, 123431.

105. Wang, C.-Y.; Zhang, X.; Zhang, Y.-J.; Chen, J.-J.; Huang, G.-X.; Jiang, J.; Wang, W.-K.; Yu, H.-Q., Direct generation of hydroxyl radicals over bismuth oxybromide nanobelts with tuned band structure for photocatalytic pollutant degradation under visible light irradiation. *Applied Catalysis B: Environmental* **2018,** *237*, 464-472.

106. Xia, Y.; Su, J.; He, Z., Z-Scheme charge separation in $Bi_{24}O_{31}Br_{10}/SrTiO_3$ nanocomposites for degradation of methyl orange. *Journal of Electronic Materials* **2019,** *48*, 3890-3899.

107. Liu, D.; Yao, W.; Wang, J.; Liu, Y.; Zhang, M.; Zhu, Y., Enhanced visible light photocatalytic performance of a novel heterostructured $Bi_4O_5Br_2/Bi_{24}O_{31}Br_{10}/Bi_2SiO_5$ photocatalyst. *Applied Catalysis B: Environmental* **2015,** *172*, 100-107.

108. Cao, C.; Xu, H.; Wang, D.; Fang, Z.; Yu, J.; Wang, Y., Facile Fabrication of $Bi_{24}O_{31}Br_{10}$ Nanosheets with Phosphorus Sulfide Quantum Dots for Highly Photocatalytic Treating Organic Dyes. *European Journal of Inorganic Chemistry* **2023,** *26* (22), e202300035.

109. Li, Y.; Xu, K.; Hu, H.; Jia, L.; Zhang, Y.; Zhuoga, C.; Yang, P.; Tan, X.; Guo, W.; Hao, W., Bi vacancy simultaneous manipulation of bulk adsorption and carrier utilization to replenish the mechanism of Cr(VI) photoreduction at universal pH. *Chemical Engineering Journal* **2022,** *450*, 138106.

110. Wan, J.; Yang, W.; Liu, J.; Sun, K.; Liu, L.; Fu, F., Enhancing an internal electric field by a solid solution strategy for steering bulk-charge flow and boosting photocatalytic activity of $Bi_{24}O_{31}Cl_xBr_{10-x}$. *Chinese Journal of Catalysis* **2022,** *43* (2), 485-496.

111. Marks, M.; Jeppesen, H. S.; Lock, N., Tuneable phase, morphology, and performance of bismuth oxyhalide photocatalysts via microwave-assisted synthesis. *ACS Applied Materials & Interfaces* **2022,** *14* (20), 23496-23506.

112. Yu, J.; Cui, M.; Liu, X.; Chen, Q.; Wu, Y.; He, Y., Preparation of novel $AgBr/Bi_3O_4Br$ hybrid with high photocatalytic activity via in situ ion exchange method. *Materials Letters* **2017,** *193*, 73-76.

113. Huang, X.; Zhang, H.; Zhao, J.; Jiang, D.; Zhan, Q., Carbon quantum dot (CQD)-modified Bi_3O_4Br nanosheets possessing excellent photocatalytic activity under simulated sunlight. *Materials Science in Semiconductor Processing* **2021,** *122*, 105489.

114. Liu, X.; Jiang, X.; Chen, Z.; Yu, J.; He, Y., Preparation of $Bi_3O_4Br/BiOCl$ composite via ion-etching method and its excellent photocatalytic activity. *Materials Letters* **2018,** *210*, 194-198.

115. Zhou, R.; Zhang, D.; Wang, P.; Huang, Y., Regulation of excitons dissociation in AgI/Bi_3O_4Br for advanced reactive oxygen species generation towards photodegradation. *Applied Catalysis B: Environmental* **2021,** *285*, 119820.

116. Di, J.; Xia, J.; Chisholm, M. F.; Zhong, J.; Chen, C.; Cao, X.; Dong, F.; Chi, Z.; Chen, H.; Weng, Y. X., Defect-tailoring mediated electron–hole separation in single-unit-cell Bi_3O_4Br nanosheets for boosting photocatalytic hydrogen evolution and nitrogen fixation. *Advanced Materials* **2019,** *31* (28), 1807576.

117. Zhou, Q.; Jiang, J., Bi_3O_4Br nanoplates as an efficient piezo-photocatalyst for organic dye degradation. *Modern Physics Letters B* **2021,** *35* (07), 2150119.

118. Tian, J.; Wei, L.; Hu, J.; Lu, J., Boosting reactive oxygen species generation over $Bi_3O_4Br/CuBi_2O_4$ by activating peroxymonosulfate under visible light irradiation. *Separation and Purification Technology* **2022,** *289*, 120794.

119. Chen, B.; Hou, Y.; Li, H.; Gao, H.; Fu, H.; Liao, F.; Zhang, J.; Liao, Y., Self-sacrificed BiOBr template-

assisted synthesis of α-Bi_2O_3/Bi_3O_4Br heterojunctions with oxygen vacancies for enhanced photocatalytic nitrogen fixation. *Journal of Colloid and Interface Science* **2023,** *652*, 1857-1866.

120. Hu, H.; Jin, J.; Xu, M.; Xu, C.; Cheng, Y.; Ji, W.; Ding, Z.; Shao, M.; Wan, Y., Novel Z-scheme Bi_3O_4Br/NH_2-MIL-125(Ti) composite for efficient photocatalytic degradation of tetracycline. *Optical Materials* **2023,** *135*, 113262.

121. Ji, J.; Sun, X.; He, W.; Liu, Y.; Duan, J.; Liu, W.; Nghiem, L. D.; Wang, Q.; Cai, Z., Built-in electric field enabled in carbon-doped Bi_3O_4Br nanocrystals for excellent photodegradation of PAHs. *Separation and Purification Technology* **2022,** *302*, 122066.

122. Sun, X.; Li, L.; Jin, S.; Shao, W.; Wang, H.; Zhang, X.; Xie, Y., Interface boosted highly efficient selective photooxidation in Bi_3O_4Br/Bi_2O_3 heterojunctions. *Escience* **2023,** *3* (2), 100095.

123. Song, Y.; He, W.; Sun, X.; Lei, J.; Nghiem, L. D.; Duan, J.; Liu, W.; Liu, Y.; Cai, Z., C-doped Bi_3O_4X nanosheets with self-induced internal electric fields for pyrene degradation: Effects of carbon and halogen element type on photocatalytic activity. *Separation and Purification Technology* **2023,** *323*, 124426.

124. Xu, H.; Hu, Y.; Huang, D.; Lin, Y.; Zhao, W.; Huang, Y.; Zhang, S.; Tong, Y., Glucose-induced formation of oxygen vacancy and Bi-metal comodified Bi_5O_7Br nanotubes for efficient performance photocatalysis. *ACS sustainable chemistry & engineering* **2019,** *7* (6), 5784-5791.

125. Wang, Y.; Wang, Q.; Zhang, H.; Wu, Y.; Jia, Y.; Jin, R.; Gao, S., CTAB-assisted solvothermal construction of hierarchical Bi_2MoO_6/Bi_5O_7Br with improved photocatalytic performances. *Separation and Purification Technology* **2020,** *242*, 116775.

126. Su, Y.; Ding, C.; Dang, Y.; Wang, H.; Ye, L.; Jin, X.; Xie, H.; Liu, C., First hydrothermal synthesis of Bi_5O_7Br and its photocatalytic properties for molecular oxygen activation and RhB degradation. *Applied Surface Science* **2015,** *346*, 311-316.

127. Wang, S.; Hai, X.; Ding, X.; Chang, K.; Xiang, Y.; Meng, X.; Yang, Z.; Chen, H.; Ye, J., Light-switchable oxygen vacancies in ultrafine Bi_5O_7Br nanotubes for boosting solar-driven nitrogen fixation in pure water. *Advanced Materials* **2017,** *29* (31), 1701774.

128. Bai, Y.; Shi, X.; Wang, P.; Wang, L.; Xie, H.; Li, Z.; Qu, L.; Ye, L., Synthesis of one-dimensional $Bi_5O_7Br_{0.5}I_{0.5}$ solid solution for effective real oilfield wastewater treatment via exciton photocatalytic process. *Journal of the Taiwan Institute of Chemical Engineers* **2018,** *91*, 358-368.

129. Hua, J.; Feng, S.; Ma, C.; Huang, H.; Wei, K.; Dai, X.; Wu, K.; Wang, H.; Bian, Z., An innovative 2D/2D Bi_5O_7Br/NiFe-LDH Z-scheme heterojunction for enhanced photoreduction CO_2 activity. *Journal of Environmental Chemical Engineering* **2023,** *11* (6), 111290.

130. Mao, D.; Yang, S.; Hu, Y.; He, H.; Yang, S.; Zheng, S.; Sun, C.; Jiang, Z.; Qu, X.; Wong, P. K., Efficient CO_2 photoreduction triggered by oxygen vacancies in ultrafine Bi5O7Br nanowires. *Applied Catalysis B: Environmental* **2023,** *321*, 122031.

131. Guo, N.; Cao, X.; Li, Q.; Han, Y.; Li, H.; Yuan, Y., Oxygen-vacancy-rich Ag/Bi_5O_7Br nanosheets enable improved photocatalytic NO removal and oxygen evolution under visible light exposure. *Advanced Powder Technology* **2023,** *34* (1), 103927.